Human Molecular Genetics, 2003, Vol. 12, No. 10 **1131–1142**
DOI: 10.1093/hmg/ddg124

Identification of a novel lipase gene mutated in lpd mice with hypertriglyceridemia and associated with dyslipidemia in humans

Xiao-Yan Wen[1,7,*], Robert A. Hegele[2], Jian Wang[2], Ding Yan Wang[1], Joseph Cheung[3], Michael Wilson[4], Maryam Yahyapour[1], Yahong Bai[1], Lihua Zhuang[1], Jennifer Skaug[3], T. Kue Young[5], Philip W. Connelly[6], Ben F. Koop[4], Lap-Chee Tsui[3,†] and A. Keith Stewart[1,7]

[1]Department of Experimental Therapeutics, Toronto General Research Institute, Toronto General Hospital, University Health Network, Toronto, Ontario, Canada, [2]Robarts Research Institute, London, Ontario, Canada, [3]The Hospital for Sick Children Research Institute, Toronto, Ontario, Canada, [4]University of Victoria, Victoria, British Columbia, Canada, [5]Department of Public Health Sciences, University of Toronto, Toronto, Ontario, Canada, [6]Departments of Laboratory Medicine and Pathobiology, University of Toronto and St Michael's Hospital, Toronto, Ontario, Canada and [7]McLaughlin Center for Molecular Medicine, Toronto, Ontario, Canada

Received January 3, 2003; Revised February 28, 2003; Accepted March 12, 2003

Triglyceride (TG) metabolism is crucial for whole body and local energy homeostasis and accumulating evidence suggests an independent association between plasma TG concentration and increased atherosclerosis risk. We previously generated a mouse insertional mutation *lpd* (lipid defect) whose phenotype included elevated plasma TG and hepatic steatosis. Using shotgun sequencing (~500 kb) and bioinformatics, we have now identified a novel lipase gene *lpdl* (*lpd* lipase) within the *lpd* locus, and demonstrate the genetic disruption of exon 10 of *lpdl* in the *lpd* mutant locus. *lpdl* is highly expressed in the testis and weakly expressed in the liver of 2-week old mice. Human *LPDL* cDNA was subsequently cloned, and was found to encode a 460AA protein with 71% protein sequence identity to mouse *lpdl* and ~35% identity to other known lipases. We next sequenced the human *LPDL* gene exons in hypertriglyceridemic subjects and normal controls, and identified seven SNPs within the gene exons and six SNPs in the adjacent introns. Two hypertriglyceridemic subjects were heterozygous for a rare DNA variant, namely 164G>A (C55Y), which was absent from 600 normal chromosomes. Two other coding SNPs were associated with variation in plasma HDL cholesterol in independent normolipidemic populations. Using bioinformatics, we identified another novel lipase designated LPDLR (for 'LPDL related lipase'), which had 44% protein sequence identity with LPDL. Together with the phospholipase gene *PSPLA1*, *LPDL* and *LPDLR* form a new lipase gene subfamily, which is characterized by shortened lid motif. Study of this lipase subfamily may identify novel molecular mechanisms for plasma and/or tissue TG metabolism.

INTRODUCTION

Lipases hydrolyze a wide range of esterified FA species within triglyceride (TG), and are often active against other substrates, such as phospholipids (PLs). At least 20 lipases or lipase-like molecules have been given names and accession numbers in OMIM (www.ncbi.nlm.nih.gov/entrez/query). These lipases have been characterized based upon factors such as their anatomical distribution, localization intra- or extra-cellularly, substrate specificity, and or homology with other lipases (1). For instance, lipases that function within the plasma compartment, anchored to endothelium by heparan sulfate proteoglycans, include, in order from most-to-least-potent TG lipase activity, and least-to-most-potent PL lipase activity, lipoprotein

*To whom correspondence should be addressed at: Department of Experimental Therapeutics, Toronto General Research Institute, Toronto General Hospital, Room 410, 67 College Street, Toronto, Ontario, Canada M2M 1E1. Tel: +1 4163403713; Fax: +1 4163403453; Email: x.wen@utoronto.ca
†Present address: The University of Hong Kong, Pokfulam Road, Hong Kong.

lipase (LPL), hepatic lipase (HL), and endothelial lipase (EL) (2–5). Other lipases are non-secreted and have predominantly intracellular hydrolytic activity, such as hormone sensitive lipase (HSL) and lysosomal acid lipase (LAL) (6,7). The activity of some other lipases is extracorporeal, such as that of pancreatic lipase (PNLIP) within the intestine.

Naturally occurring loss-of-function mutations in *LPL* cause chylomicronemia (8,9); some *LPL* single-nucleotide polymorphisms (SNPs) are fairly consistently associated with metabolic and cardiovascular phenotypes (10) and *LPL* knock-out and transgenic mice have instructive phenotypes involving the expected alterations in plasma TG and HDL (11). Similarly, naturally occurring loss-of-function mutations in *HL* cause a complex hyperlipidemia with early atherosclerosis (12); some *HL* SNPs, especially −514C>T, are consistently associated with metabolic and cardiovascular disease phenotypes (9,13), and *HL* knock-out and transgenic mice have instructive phenotypes that reflect the human phenotypes (14). In contrast, neither naturally occurring human mutations, nor induced murine mutations in *EL* have yet been reported, although several common SNPs have been associated with variation in plasma concentrations of HDL cholesterol (15). Mild to moderate hypertriglyceridemia (Fredrickson type IV) with low HDL cholesterol is among the most common hyperlipidemia seen in many lipid clinics, but most patients have no mutation in either *LPL* or *HL*. Thus, it remains important to identify new candidate genes for TG metabolism.

We previously identified a mouse transgenic insertional mutation, *lpd* (for 'lipid defect'), characterized by perinatal accumulation of TG in both plasma and liver. Molecular cloning of the transgene-flanking sequences led to mapping of the *lpd* locus to the distal part of murine chromosome 16 (16). Further mapping studies ruled out the identity of *lpd* with a recently identified phospholipase gene *ps-pla1* in the same vicinity (17). Here, we report the identification of a novel lipase gene (designated *lpdl* for lpd lipase) in the *lpd* locus and its human homolog *LPDL*. Using bioinformatics, we also identified a related lipase designated *LPDLR* (for LPDL-related lipase) with significant structure similarity. *LPDLR* has also recently been described as *LIPH* (18). Together with *PS-PLA1*, *LPDL* and *LPDLR* (*LIPH*) form a new lipase subfamily.

RESULTS

Sequencing of the *lpd* locus and bioinformatic identification of a novel lipase (*lpdl*)

Because mutant *lpd* homozygotes had hepatic steatosis and hypertriglyceridemia, we hypothesized that the murine *lpd* locus would encode a TG lipase. Since analysis of the junction sequences of the *lpd* transgene insertion locus did not yield any lipase-related sequences and the mouse genetic sequencing database was not available at that time, we chose to clone the entire wild-type *lpd* locus with bacteria artificial chromosomes (BACs) that encompassed the affected region. By screening a wild-type mouse genomic BAC library with two probes that flanked each side of the transgene, three BAC clones containing the *lpd* locus were identified. Using shotgun strategy, we sequenced one BAC clone (BAC no. O16) with ∼3-fold redundancy. Seven hundred and nineteen sequences for a total of 449 373 bp were randomly sequenced. These sequences formed 93 contigs for a total contig length of 163 372 bp. We used the BLASTX engine (www.ncbi.nlm.nih.gov) to interrogate all non-redundant GenBank sequences with the 93 contigs and identified a fragment in contig no. 6 that had significant homology to a portion of both human and rat phosphatidylserine-specific phospholipase A1 (*PS-PLA1*) with ∼50% identity at the protein sequence level.

Following the identification of this lipase-related sequence, bioinformatic gene prediction tools were used to identify five putative exons from four contigs (nos 6, 28, 86 and 98), which translated as a continuous putative protein sequence of 261 amino acid (designated as *lpd* lipase) that includes the highly conserved Gly-Met-Ser-Leu-Gly lipase consensus sequences (Fig. 1).

Genomic structure and expression of human/mouse *LPDL*/*lpdl* and genetic disruption of the *lpdl* gene in the *lpd* insertional locus

Using the mouse *lpdl* exon sequences to BLAST, we identified a genomic sequence of 340 kb (AP001660) on human chromosome 21q with significant homology to the mouse *lpdl* gene. Ten DNA fragments from this genomic sequence were further characterized as exons of the human *LPDL* gene. The exon–intron boundaries were determined using a combination of analysis with exon/intron consensus sequences, bioinformatic gene prediction tools and alignment with the cloned human cDNA sequences (Table 1). The exon sizes of human *LPDL* gene range from 90 to 386 bp and they span a genomic region >100 kb. The largest intron, intron 9, spans 35 kb and the smallest intron, intron 5, spans ∼1 kb (Table 1). Start and stop codons are located in exons 1 and 10, respectively, and lipase consensus sequence G × S × G is encoded from exon 3. Exons 4, 5 and 6 span the most conserved lipase regions, including the lid sequences and two of three active residues within the triad structure for catalytic activity.

Using 5′ RACE, sequencing, searching mouse genetic databases and bioinformatic gene prediction, we identified a continuous mouse genomic fragment of 110 kb, which contained all 10 putative exons of the mouse *lpdl* gene. When aligning the mouse *lpdl* sequences with the human genomic *LPDL* sequences, nine of 10 exons were within the conserved peaks with >75% sequence identity (Fig. 2). Within the ∼5 kb region before exon 1, there was another cluster of peaks with sequence identity of 50–75% which may represent the conserved promoter sequences for the gene and regulatory elements.

Since the identified lipase-like gene was a logical candidate for the *lpd* phenotype, we next confirmed that the transgene insertion in the *lpd* locus disrupted the *lpdl* lipase gene. We mapped the transgene junction clones relative to the gene structure of the mouse *lpdl* gene. One junction clone (D3) was mapped before mouse exon 10 while the other junction clone (3A) mapped after exon 10 (Fig. 2), indicating that exon 10 of the *lpdl* gene was deleted in the mutant *lpd* locus. It is perhaps of interest that ∼7 kb upstream of the *lpdl* gene, there were five conserved peaks (with >75% identity) designated as conserved nucleotide sequences (CNS), which may represent another gene (Fig. 2). A

A Shotgun Sequencing

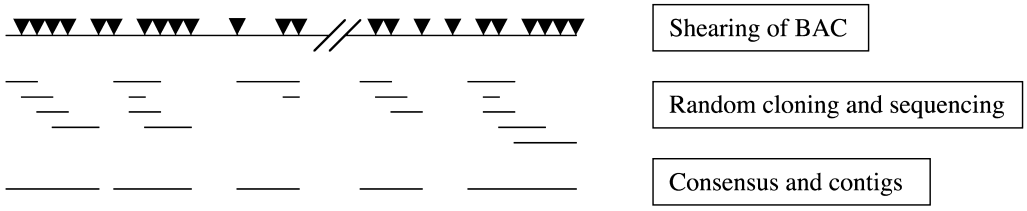

1,394 clones sequenced for total of 449,373 bp
93 contigs generated for contig length of 163,372 bp

B Identification of putative exons of mouse *lpdl* gene

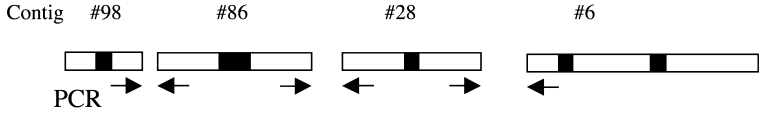

C Mouse lpdl protein sequences predicted from putative exons

VKINLLMYSRGNAKCAEPLFESNNSLNTRFNPAKKTVWIIHGYRPFGSTPVWLSR
FTKAFLKQEDVNLIVVDWNQGATTFMYSRAVRNTRRVAEILRETIENLLIHGASL
DNFHFIGMSLGAHISGFVGKIFHGQLGRITGLDPAGPQFSRKPSNSRLYYTDAKFV
DVIHTDIKSLGIGEPSGHIDFYPNGGKHQPGCPTSIFSGTNFIKCDHQRAIYLFLAA
FETSCNFVSFPCRSYKDYKNGLCVDCGNLYKDSCPRLG

Figure 1. Shotgun sequencing of BAC Clone and identification of *lpdl* gene exons and putative protein sequences. (**A**) Sequencing of BAC clone BAC no. O16 included shearing of the BAC DNA, random cloning, sequencing and multiple sequence alignment to generate consensus sequences and contigs. (**B**) Five exons were identified from contig nos 98, 86, 28 and 6. (**C**) Mouse lpdl protein sequences translated from putative exons.

Table 1. Exon–intron boundaries of human *LPDL*

Exon	Size (bp)	5′ Boundary	3′ Boundary	Intron	Size (kb)
1	106	...GAGTTACGGA	GTGAGATCTGgtaagatatt	1	21
2	386	cttatttcagATAATAAAAG	AAATCTTTTGgtaagtctgg	2	3
3	109	ttaattgcagAAGCATGGTG	AGAATAACAGgtaaaattat	3	4
4	102	tgctttccagGTCTTGACCC	GACTCCAATGgtaacaaatc	4	15
5	90	ttcttctcagGTTTAGGCAT	ATTTTCTCAGgtatactgac	5	1
6	168	aacccttaagGAATTCAATT	CCTCGGCTGGgtaagagaga	6	2
7	105	caaatctcagGTTATCAAGC	CCATTCTGTAgtaagttatt	7	10
8	112	tattttgtagCCTATTATTT	GGCTTTATGAgtaagtaaaa	8	10
9	177	ttctctctagAAAGAACAAA	ACCCAGAAAGgtaagaaaat	9	35
10	206	tctttctcagACCACCACTT	CTATTTCTTGG...		

TBLASTX search against GenBank with the CNS sequences identified a novel putative protein with high sequencing homology to human putative RNA-binding protein 11 (P57052) (data not shown).

With the availability of murine *lpdl* exon sequences, we next sought to identify mouse and human ESTs in the published genetic databases, however no ESTs with significant homology were found. Northern blot analysis was then performed on mouse multitissue blots using probes generated from predicted exon sequences of the mouse *lpdl* genomic BAC clone. We detected a ~2 kb band in testis RNA but not in any other adult mouse tissues examined, including heart, brain, spleen, lung, liver, skeleton muscle and kidney (Fig. 3A-a). By RNA *in situ* hybridization, the *lpdl* gene was found to be highly expressed in the testis (Fig. 3B-b) and weakly expressed in the hepatocytes of 2-week-old mice (Fig. 3B-d). In the testis of adult mice, *lpdl* was

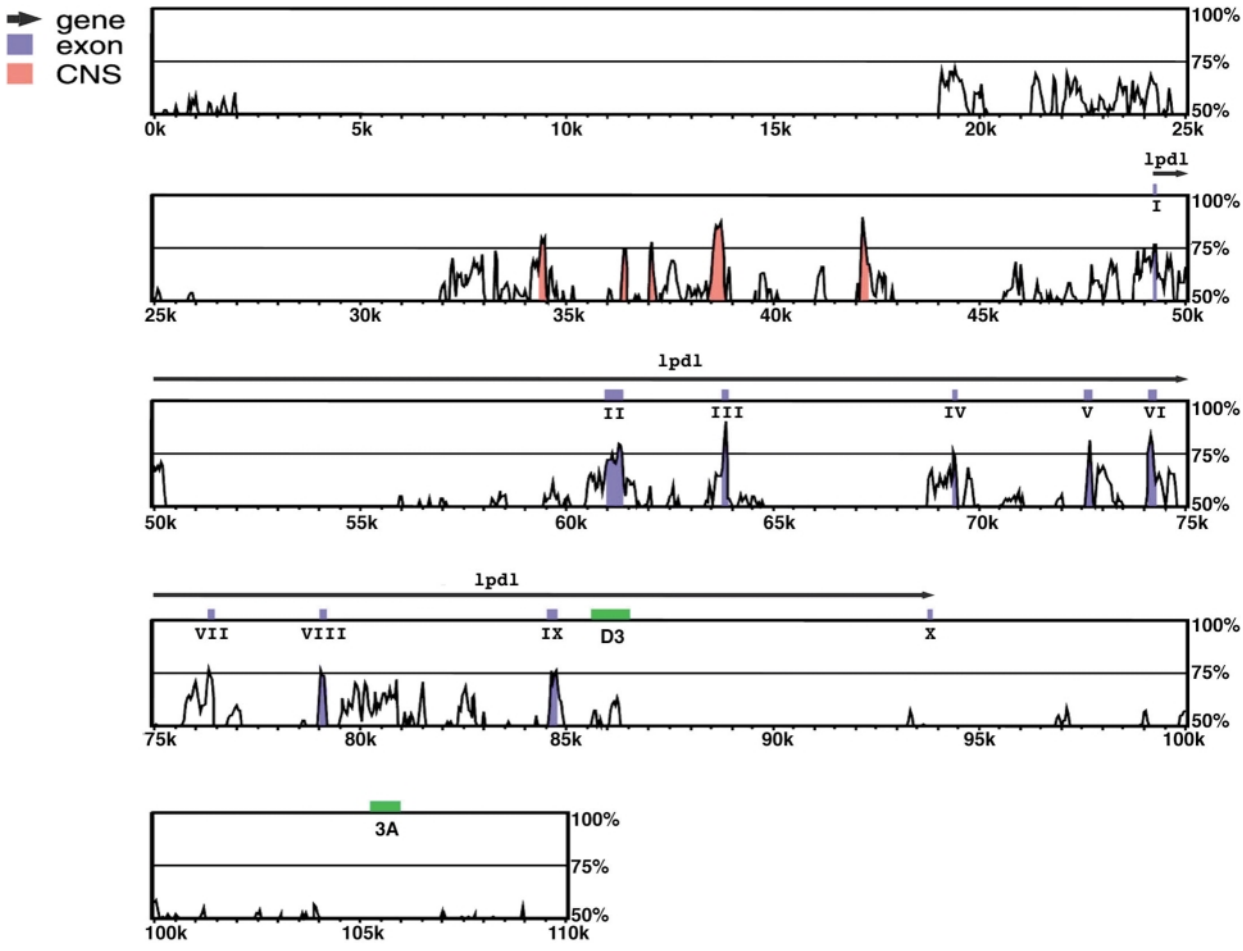

Figure 2. Comparison of 110 kb of mouse *lpd* genomic sequences with orthologous human genomic sequences. Each window represents 25 kb of orthologous DNA sequence displayed using the program VISTA (www-gsd.lbl.gov/vista). Peaks represent the percentage of sequence identity. The arrow indicates the direction of gene transcription. Blue segments represent the exons of the gene while red segments represent CNS which may be putative exons of another gene. The flanking clones of the transgene insertion, D3 and 3A, were mapped before and after exon 10, respectively, suggesting exon 10 is deleted in mutant *lpd* locus.

expressed in the cytoplasm of primary spermatocytes but not in the matured sperm or in Leydig cells (Fig. 3B-f). Similar to murine *lpdl* expression pattern, northern blotting showed that human *LPDL* was expressed in testis (Fig. 3A-b) but was not detected in any other human tissues including brain, liver, heart, skeleton muscle, lung and intestines (data not shown).

Identification of human *LPDL* and murine *lpdlr* (lpdl related lipase) gene

Using mouse *lpdl* gene fragments as probes to screen a human testis large insert cDNA library (Clontech), four positive clones were identified. Sequencing of these clones revealed a cDNA of 1685 bp, with an open reading frame (ORF) of 1383 bp, a start codon (ATG) at nt 78 and a stop codon (TAG) at nt 1640. The ORF encodes a human *LPDL* protein of 460 amino acids (Fig. 4). A hydrophobic leader sequence with a putative cleavage site after amino acid residue 15 was predicted by the SPScan program of SeqWeb Wisconsin GCG Package. The lipase consensus sequence G × S × G was found with an active serine at amino acid residue 159. DNA sequence analysis suggested the existence of two additional active residues, Asp183 and His258, which are predicted to form a catalytic triad with Ser159 (19). A lipase lid sequence, which may determine substrate specificity (20), was identified between two cysteines at residues 238 and 251. Seven conserved cysteines at residues 55, 238, 251, 275, 286, 289 and 297 could participate in disulfide bridge formation (21). Other conserved cysteines include Cys11 and Cys455 (Fig. 4).

Using lpdl protein sequence to BLAST-search against the translated EST database, we identified a mouse EST (BG868436, from salivary gland) which translated to another novel lipase with significant homology to *lpdl*. We named this novel lipase as *lpdl*-related lipase or *lpdlr*. Sequencing of BG868436 revealed a cDNA of 2155 bp in length with ORF starting from nucleotide 78 and stopping at nucleotide 1640. The ORF encodes a mouse lpdlr protein of 451 amino acids (Fig. 4). The lipase consensus sequence G × S × G was found with an active serine at amino acid residue 154. Alignment analysis suggested that, for the putative catalytic triad, Asp178 and Ser154 were conserved (19), but the normally conserved histidine residue within the triad was replaced by Tyr253

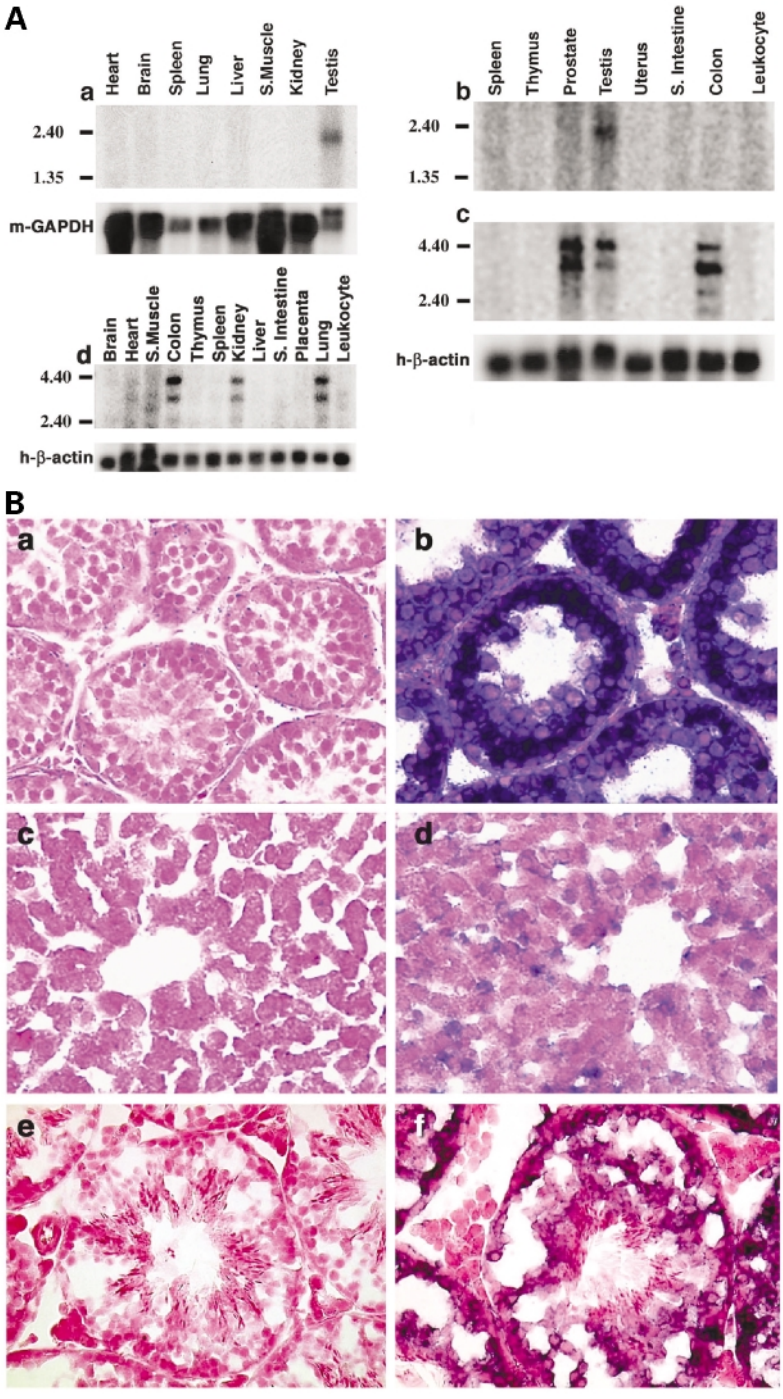

Figure 3. Gene expression and tissue distribution of *LPDL* and *LPDLR*. (**A**) By northern blot analysis, mouse and human *LPDL* genes are expressed in testis tissue (**a** and **b**, respectively); the human *LPDLR* is expressed in prostate, testis, colon, kidney and lung tissue with four differently sized transcripts detected (**c** and **d**). (**B**) By non-radiation RNA *in situ* hybridization with anti-sense probe, mouse *lpdl* is expressed strongly in testis (**b**) and weakly in the liver (**d**) in 2 week-old mice as compared with control tissue sections hybridized with sense probe (**a** and **c**). In adult mice (**e** and **f**), *lpdl* expression is detected in the cytoplasm of primary spermatocytes but not in the matured sperm or Leydig cells between the seminiferous tubules (f).

(Fig. 4). A human EST (AW845952) harbored part of the *LPDLR* gene. Northern blot hybridization with labeled AW45952 fragment as probe demonstrated that the human *LPDLR* gene was highly expressed in lung, colon, prostate, kidney and testis with four different sized isoforms ranging from 2 to 4 kb (Fig. 3A-c and A-d).

With the availability of genomic and/or cDNA sequences of both human and mouse genes of *LPDL* and *LPDLR*, we

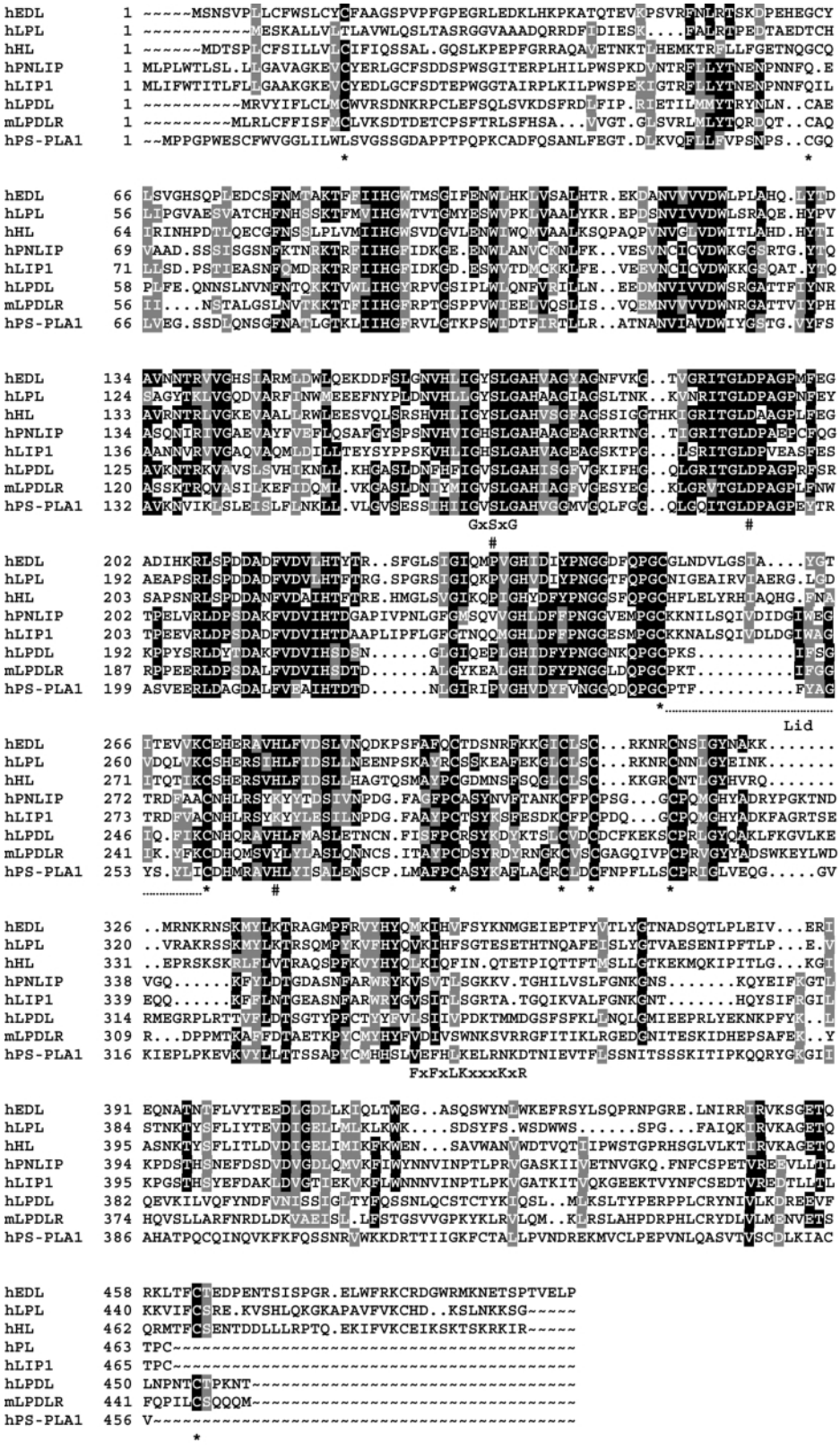

Figure 4. Multiple sequence alignment of human LPDL and mouse LPDLR with other TG lipases and PS-PLA1. Triglyceride lipases and PS-PLA1 demonstrate significant sequence homology which includes the conserved lipase consensus sequence G × S × G, multiple cysteine residues that may be required for disulfide bridge formation (undermarked by an asterisk), and three residues of catalytic triad (undermarked by a hash). The lid sequences of hLPDL and mLPDLR are similar to hPS-PLA1 with 12 amino acids in length, which is much shorter than the other TG lipases. PS-PLA1 carries a modified phosphatidylserine-binding motif xxFxLKxxxxKx which is not seen in TG lipases.

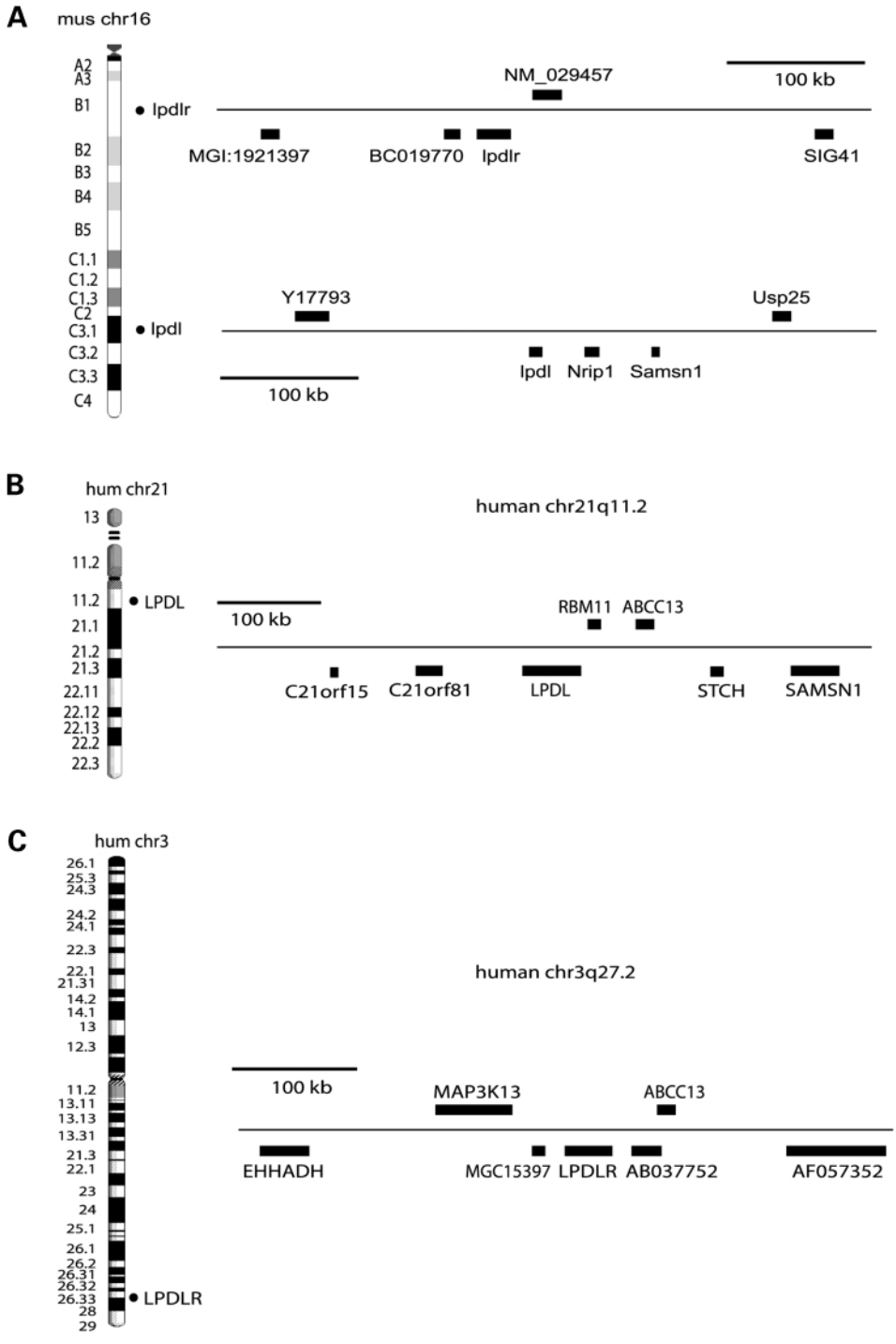

Figure 5. Chromosomal location and the adjacent gene map of mouse and human LPDL and LPDLR genes. Chromosomal locations of LPDLs and LPDLRs were identified by using the UCSC Genome Browser (http://genome.ucsc.edu). (**A**) Both mouse *lpdl* and *lpdlr* genes map to murine chromosome 16 in B1 and C3.1 region, respectively. Human *LPDL* maps to chromosome 21q11.2 (**B**) while *LPDLR* is located in the distal part of chromosome 3 (3q27.2) (**C**).

identified their chromosome locations by using the UCSC Genome Browser (http://genome.ucsc.edu). As shown, both mouse *lpdl* and *lpdlr* genes map to murine chromosome 16 residing in B1 and C3.1 region, respectively (Fig. 5A). *Nrip1* and *Samsn1* map within 100 kb distal to *lpdl* while *lpdlr* is located between BC019770 and NM_029457. Human *LPDL* maps to chromosome 21q11.2 and is within 100 kb centromeric to *STCH* and *SAMSN1* (Fig. 5B). Human *LPDLR* is located in the distal part of chromosome 3 (3q27.2) between MGC15397 and AB037752 (Fig. 5C).

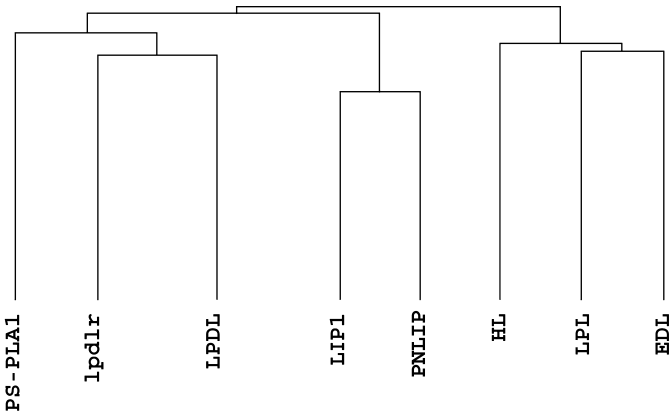

Figure 6. The multiple sequence alignment dendrogram of members in the lipase family. Lipases and phospholipase PS-PLA1 sequences are compared by SeqWeb peptide PileUp software from Wisconsin GCG Package. Human LPDL and mouse LPDLR demonstrate higher sequence homology with PS-PLA1 and thus are clustered together and they form a subfamily.

LPDL and *LPDLR* belong to a novel subfamily

Alignment of human *LPDL* and mouse *lpdlr* protein sequences with other human lipases revealed significant structural conservation (Fig. 4). The 'catalytic triad', as well as the lipase consensus sequences G × S × G are conserved in all TG lipases and PS-PLA1. Among the highly conserved cysteine residues required in TG lipase for tertiary structure formation (21), seven appear to be conserved in both LPDL and lpdlr proteins (Fig. 4). Interestingly, the glycine G364 of LPDL is conserved in all TG lipases, but not in PS-PLA1 (Fig. 4). Using algorithm analysis (22), LPDL showed 36, 34, 32, 31 and 31% amino acid identity to human endothelial lipase (LIPG), PNLIP, HL, pancreatic lipase related protein 1 (LIP1) and LPL, respectively. Human LPDL protein exhibits 44% amino acid identity to mouse lpdlr protein, and 71% amino acid identity to its mouse homolog lpdl (from partial lpdl sequences). Interestingly, human LPDL also demonstrates relatively high (∼34% amino acid) sequence identity to phospholipase PS-PLA1.

The lid domain plays a crucial role in determining lipase substrate specificity (20,23). The lid in both human LPDL and mouse lpdlr is composed of 12 amino acids, which is much shorter than those found in human PNLIP, LIP1, EDL, LPL and HL (23, 23, 19, 22 and 22 residues, respectively; Fig. 4). Interestingly, both hLPDL and mLPDLR lid sequences show higher homology to the lid of PS-PLA1, which is also 12 amino acids in length (Fig. 4). The multiple sequence alignment dendrogram shows that *LPDL*, *LPDLR* and *PS-PLA1* share higher protein sequences homology and are clustered together (Fig. 6), suggesting they form a subfamily within the lipase gene family.

LPDL SNPs and association with plasma lipoproteins

Since the mouse *lpd* mutation had both disrupted *lpdl* and high plasma TG, we considered that *LPDL* gene variation in humans might contribute to dyslipidemia. We addressed this hypothesis in two ways. First, from genomic DNA we directly sequenced *LPDL* exons of 60 non-diabetic Caucasians with moderate to severe hypertriglyceridemia (mean ± SEM untreated TG 12.1 ± 8.5 mmol/l; age 55 ± 12 years) who had no obvious secondary cause of hyperlipidemia, and 10 matched normolipidemic Caucasian controls (untreated TG 1.1 ± 0.3 mmol/l). The hypertriglyceridemic subjects had previously been shown to have no mutation in *LPL*, *HL* or *EL*. For newly discovered SNPs, allele frequencies were determined in 80 Caucasians. We found six non-transcribed and seven transcribed SNPs, including the nonsynonymous coding SNPs C55Y, G364E, E431K and D444E (Table 2). Genotype frequencies for each SNP did not deviate significantly from Hardy–Weinberg expectations in all samples. Mild to moderate pairwise linkage disequilibrium was observed for about half of the pairwise comparisons of *LPDL* SNP genotypes in Caucasians (data not shown). Two SNPs were further characterized in several additional samples of 80 individuals each: in African, East Indians, Chinese, Inuit and Amerindian, the frequencies for K431 were 0.57, 0.24, 0.05, 0.31 and 0.20, respectively, and the frequencies for E444 were 0.53, 0.51, 0.58, 0.69 and 0.51, respectively. Allele frequencies of coding SNPs in 186 hypertriglyceridemic Caucasian subjects (TG > 10 mmol/l) and 232 matched Caucasian controls (TG < 1 mmol/l) were compared, and none was found to be significantly different between samples. However, heterozygosity for C55Y was found only in the Caucasian hypertriglyceridemic patients (2/186 versus 0/232), suggesting that this might be a rare mutation associated with hypertriglyceridemia.

Next, we tested for associations of SNP genotypes with plasma lipoproteins in three unrelated samples using our established approach (24–26). Two independently ascertained, unrelated samples of healthy, normolipidemic Caucasians (174 and 161 individuals) and a well-characterized sample of healthy Inuit (208 subjects) (26) were studied. In ANOVA, dependent variables were the four plasma lipoprotein traits (TG, total, HDL and LDL cholesterol), appropriately transformed to give distributions that were not significantly different from normal. Correction was made for age, sex and body mass index by including these as independent covariates, along with the genotype for the coding SNPs only, assuming dominant, co-dominant and recessive models for each minor allele, as described (26). Seven significant associations were found with plasma lipoproteins (Table 3). At least one *LPDL* SNP genotype was associated with variation in HDL cholesterol in all three samples (Table 3). Also, *LPDL* SNP genotypes were associated with variation in LDL cholesterol in both Caucasian samples (Table 3).

DISCUSSION

Characterization of insertional mutations has been a useful strategy for identifying novel genes, since the mutated locus becomes tagged by the transgene, which provides a unique marker for cloning (27). The fortuitous observation of plasma and tissue TG disturbances in the insertional mutation of *lpd* transgenic mouse provided an important clue that the disrupted *lpd* locus on murine chromosome 16 contained a gene required

Table 2. *LPDL* SNPs and allele frequencies

Location	Amino acid	Nucleotide	Allele frequencies (Caucasian)
A. Non-transcribed LPDL SNPs			
Intron 1		41 nt 5′ to exon 2 C>T	T: 0.14
Intron 2		74 nt 5′ to exon 3 C>T	T: 0.25
Intron 4		49 nt 3′ to exon 4 A>G	G: 0.32
Intron 5		16 nt 5′ to exon 6 T>C	C: 0.02
Intron 9		46 nt 3′ to exon 9 G>A	A: 0.35
3′ to ORF		nt+146 G>T	T: 0.18
B. Transcribed LPDL SNPs			
Exon 1		−54C>T	T: 0.20
Exon 2	C55Y	164G>A	Only in hypertriglyceridemic subjects
Exon 3	S159	477C>T	T: 0.25
Exon 8	G364E	1091G>A	A: 0.03
Exon 9	E431K	1291G>A	A: 0.34
Exon 10	D444E	1332C>A	A: 0.55
3′ UTR		+80G>A	A: 0.43

SNPs were identified by direct sequencing of *LPDL* exons in 60 hypertriglyceridemic Caucasian subjects. SNP allele frequencies were determined in 80 Caucasian subjects.

Table 3. Summary of significant ($P < 0.05$) quantitative lipoprotein associations with *LPDL* SNPs

Sample	*n*	SNP name	Trait	Model	*P*-value	Adjusted mean ± SEM for genotypes
Caucasian sample 1	174	477C>T	log HDL-C	Dominant	0.019	C/C: 0.049 ± 0.012 mmol/l C/T and T/T: 0.006 ± 0.015 mmol/l
			root LDL-C	Dominant	0.020	C/C: 1.80 ± 0.04 mmol/l C/T and T/T: 1.64 ± 0.05 mmol/l
		IVS2-74C>T	log HDL-C	Dominant	0.026	C/C: 0.050 ± 0.014 mmol/l C/T and T/T: 0.007 ± 0.014 mmol/l
			root LDL-C	Dominant	0.012	C/C: 1.79 ± 0.04 mmol/l C/T and T/T: 1.63 ± 0.05 mmol/l
Caucasian sample 2	161	IVS2-74C>T	log HDL-C	Dominant	0.019	C/C: 0.095 ± 0.019 mmol/l C/T and T/T: 0.034 ± 0.016 mmol/l
			root LDL-C	Dominant	0.005	C/C: 1.83 ± 0.08 mmol/l C/T and T/T: 1.54 ± 0.06 mmol/l
Inuit	208	D444E	log HDL-C	Recessive	0.032	D/D and D/E: 0.23 ± 0.03 mmol/l E/E: 0.31 ± 0.03 mmol/l

n, number of subjects; SNP, single nucleotide polymorphism; adjusted mean, mean value adjusted for age, sex and obesity; SEM, standard error of the mean; log, natural logarithm, HDL-C, plasma high density lipoprotein cholesterol concentration; root, square root; LDL-C, plasma low density lipoprotein cholesterol concentration.

in lipid metabolism. We report here the cloning of a novel lipase gene *lpdl* within the *lpd* locus. Mapping of the transgene insertion junction sequences with the wild-type *lpd* sequences revealed that exon 10 of *lpdl* is deleted in the *lpd* mutant locus. Mutation screening of the human *LPDL* gene in patients with hypertriglyceridemia suggests that a rare missense mutation (C55Y) may be associated with elevated TG. Other *LPDL* SNPs were associated with variation in HDL and LDL cholesterol in three independent samples. Using bioinformatic tools, we also identified another novel lipase, called LPDLR (or LIPH). Based on their significant sequence homology and conservation of the functional domains, we propose that LPDL, LPDLR and PS-PLA1 form a gene subfamily.

The lipase consensus sequence G × S × G is conserved in most TG lipases and PS-PLA1, as Ser forms a catalytic triad with His and Asp that mimics the catalytic triad of trypsin (19,23). In human *LPDL*, sequence alignment suggests that the catalytic triad consists of Ser-159, Asp-183 and His-258, whereas in mouse lpdlr, the triad consists of Ser-154, Asp-178 and Tyr-253, which replaces the histidine residue with tyrosine. The tyrosine in this functional site is also observed in mouse lpdl (data not shown). Interestingly, the PNLIP and LIP1 utilize Lys(k) instead of His in this position, indicating His is less conserved than the Ser and Asp in the triad (Fig. 4).

Most TG lipases, like LPL and HL, also display some degree of phospholipase activity. The lid sequences which form a surface loop by a disulfide bridge of two cysteines are reported to determine substrate specificity (Fig. 4). While the lid of LPL confers preferential triglyceride hydrolysis, the lid of HL augments more phospholipase activity (20). LPDL, lpdlr and

PS-PLA1 share a shortened lid structure (12 amino acids). Assuming LPDL and LPDLR are TG lipases, elements other than the lid must determine their TG substrate specificity, since PS-PLA1 was reported neither to hydrolyze TG (28) nor associate with plasma TG (29). However, PS-PLA1 contains a modified phosphatidylserine-binding peptide motif xxFxLKxxxxxx resembling the consensus sequence motif FxFxLKxxxKxR (30) which is not present in LPDL and lpdlr (Fig. 4).

Like LPDL, other lipases such as EL and HSL are highly expressed in the testis, which may reflect higher TG energy metabolism (31–34). Targeted disruption of *HSL* resulted in male sterility indicating the importance of HSL expression in testis tissue (35). Whether testicular expression of *lpdl* gene is important for testis function remains to be addressed by *lpdl* gene knock-out or conditional knock-out study since the *lpd* mutation is perinatal lethal and the *lpd* mutants do not survive to mating age (16). Since the homozygous *lpd* mutants demonstrated fatty livers with extensive accumulation of TG (16), it is expected that *lpdl* gene would be expressed in the liver. Although northern blot hybridization with *lpdl* probe did not detect the expression signal in the liver, the more sensitive RNA *in situ* hybridization did detect weak expression in hepatic tissue in 2-week-old mice, supporting the hepatic phenotype in the *lpd* mutant mice. By northern analysis, human *LPDLR* is expressed in lung, kidney, prostate, testis and colon, and ESTs of mouse *lpdlr* had also been identified from salivary gland and mammary gland suggesting a role in digesting exogenous dietary TG.

The finding that the exon 10 of *lpdl* is deleted in the *lpd* mutant suggests that C-terminal sequences may participate in the substrate specificity during TG hydrolysis. Besides deletion of exon 10, other genetic rearrangements could not be ruled out because of the complexity of gene mutations, especially transgene-induced mutations. For example, the most recently characterized mutation *fld* (fatty liver dystrophy) is characterized by a deletion of 2 kb sequences eliminating exon 2 and 3, and inversion of 40 genomic sequences plus a duplication of 0.5 kb segments in 3′UTR (36). Because *lpd* mutant mice also demonstrated runting and a potential neurological defect, we cannot rule out causative defects of more than one gene. An adjacent putative RNA binding protein 5′-flanking the *lpdl* gene is a potential candidate region contributing to the complexity of the phenotype (data not shown). Other genes in the 3′ region downstream of *lpdl* gene include a putative novel gene similar to spliceosome-associated protein 49 (AF317552), a nuclear receptor interacting protein 1 (*Nrip1*) and a nuclear protein *HACS1* (*Samsn1*, AF218085) (37). A genetic knock-out of *lpdl* lipase gene is in progress to clarify whether *lpdl* gene mutation alone could result in a phenotype as described in the *lpd* insertional mutation. If more than one genes are involved in the *lpd* mutation, the phenotype of the *lpdl* gene knock-out mice may be less severe and the resulting mice could be viable.

To identify potential mutations in human *LPDL* gene that contribute to human dyslipidemias, we conducted mutation screening of *LPDL* exons in the genomic DNA of Caucasian patients with moderate to severe hypertriglyceridemia. While seven coding SNPs were discovered, only one putative mutation was identified, namely C55Y, which was present only in hypertriglyceridemic subjects. C55 is an important residue in *LPDL*, which is predicted to participate disulfide bridge formation and in determining lipase tertiary structure (21,23). C55 is also conserved in both mouse *lpdlr* and human *PS-PLA1* (Fig. 4). Therefore, the C55Y substitution may affect its function.

Results in three independent normolipidemic samples strengthen the case for association between *LPDL* SNPs and HDL cholesterol, although linkage disequilibrium with unmeasured variants at another gene remains possible. Variation in HDL cholesterol has previously been associated with SNPs in other lipases, specifically in *LPL*, *HL* and *EL* (10,13,15). The mechanisms underlying these associations are unknown, but *LPDL* appears to be a fourth lipase that is associated with variation in plasma HDL cholesterol. The absence of concomitant association of *LPDL* SNPs with plasma TG is compatible with observations from other experiments and model systems in which TG and HDL metabolism are uncoupled (9). The less consistent association of *LPDL* SNPs with LDL cholesterol will require validation in future studies. The association of *LPDL* SNPs with plasma HDL cholesterol rather than TG concentration in humans echoes the observations for EL, which despite strong sequence similarity to both the intravascular lipases LPL and HL was found by SNP analysis to be associated with HDL cholesterol rather than TG (15). Recent *in vivo* functional assessment has confirmed that EL plays a direct role in HDL metabolism, and these findings support the idea that members of the lipase family have different affinities for a range of lipoproteins (38–40). The apparently more pronounced association with TG in the mouse but HDL cholesterol in the human could also be related to species differences and the extent of functional impairment attributable to the induced murine mutation and the human SNPs, respectively. Clearly, functional assessment of *LPDL* and more intensive characterization of biochemical phenotypes in both species are required. Similarly, the less consistent association of LPDL SNPs with LDL cholesterol will require validation in future studies. Analyses using all *LPDL* SNPs described here may be helpful in future association studies with plasma lipoproteins, as advocated by some authors (41).

Since the molecular basis for moderate dyslipidemia is still unknown for the majority of subjects, identification of novel loci and genes remains and important approach to begin to fill this gap in understanding. Linkage studies (42,43) and systematic mouse mutagenesis (44) are complementary approaches to attain this goal. Characterizing *LPDL* and *LPDLR* may identify novel molecular mechanisms for plasma and/or tissue TG metabolism, perhaps leading to new therapies for dyslipidemias and atherosclerosis prevention.

MATERIALS AND METHODS

BAC cloning, sequencing and sequence data analysis

We identified BAC clones of *lpd* locus by screening a mouse 129 BAC library RPCI-22 with ^{32}P-dCTP (Amersham Pharmacia Biotech) labeled probes generated from flanking sequences of the *lpd* transgene insertion site. Three positive clones were identified. One BAC clone, BAC no. 016,

hybridized to both flanking probes and was further sequenced. For sequencing the BAC clone, a sub-library in M13mp19 was first constructed. Briefly, BAC DNA was purified using the NucleoBond Plasmid Maxi kit (Clontech), randomly sheared by nebulization, and rendered blunt by treatment with mung bean nuclease, T4 polymerase and Klenow. Fragments from 1.5 to 3 kb were size-fractionated by agarose gel electrophoresis, ligated into *Sma*I-cut M13mp19, and transformed into DH5α competent cells. Random clones were picked and single-stranded templates were purified with Qiagen M13 plates. Sequencing was carried out on ABI 377 and 373 automated DNA sequencers using fluorescently labeled dye-primer and dye-terminator chemistries (Amersham Pharmacia Biotech). Raw sequencing data were analyzed and assembled using DNAStar and PhredPhrap software.

cDNA cloning

Mouse *lpdl* gene probes corresponding to its exons were amplified by PCR from BAC DNA with oligo primers: lpd98F (GTA AAG ATA AAT CTG CTG AT), lpd98R (TCT CAA TGG TTT CTC TC) and lpd1F (TAA ATG CGA CCA TCA GAG A), lpd1R (GTC TTG GGC AGG AGT CTT T). A large-insert cDNA library (Human Testis HL5503u, Clontech, Palo Alto, CA, USA) was used to clone human *LPDL* cDNA according to the manufacturer's instructions. Briefly the λTriplEx2 phage library was plated onto 150 mm plates, transferred to nylon membranes (Amersham Pharmacia Biotech) and hybridized to ^{32}P-dCTP labeled murine *lpdl* probes. Purified λTriplEx2 phage clones were transduced into BM25.8 *E. coli* strain to promote *Cre* recombinase-mediated release and circulation of pTriplEx plasmids. The plasmid DNAs containing the human *LPDL* cDNA were purified by Qiagen Kit and sequenced with T7 primer. Human and mouse ESTs (BG868436, AW845952) of *LPDLR* were obtained from Genome Systems Inc. (St Louis, MO, USA). The DNAs were purified by Qiagen Plasmid Maxi kit (Mississauga, Ontario, Canada) and inserts sequenced with T7 and SP6 primers.

Bioinformatic analysis of DNA and protein sequences

BLAST searching of human GenBank of nucleotide sequences at the NCBI site (www.ncbi.nlm.nih.gov/BLAST/) with mouse *lpdl* sequences from BAC contigs identified a genomic sequence of 340 kb (AP001660) on human chromosome 21q which carries the human *LPDL* gene. Mouse *lpdl* genomic sequences, 110 kb, were retrieved from UCSC Genome Bioinformatics (http://genome.ucsc.edu). Comparison of 110 kb of mouse *lpd* genomic sequences with orthologous human genomic sequences was performed using the program VISTA (www-gsd.lbl.gov/vista). The EST clones of mouse and human *LPDLR* were identified by TBLASTX against the GenBank EST database with lpdl protein sequences. Analysis of nucleotide and protein sequences of mouse and human *LPDL*, *LPDLR* and other lipases was carried out using SeqWeb software (Wisconsin GCG Package). Multiple sequence alignment was performed with the SeqWeb PileUp program and shading of consensus sequence was performed with an internet BOXSHADE3.21 server (www.ch.embnet.org/software/BOX_form.html).

Northern blot analysis and RNA *in situ* hybridization

Mouse and human multiple tissue northern blots (nos. 7762-1 and 7766-1, Clontech, Palo Alto, CA, USA) were hybridized according to the manufacturer's instructions using ExpressHyb solution (Clontech, Palo Alto, CA, USA). Probes were labeled with random priming using ^{32}P-dCTP. Hybridized filters were exposed to X-ray film overnight or analyzed with a Bio-Rad phospho-imager system Molecular Imager FX using Quantity One software. RNA *in situ* hybridization was performed on sections as described (45). Briefly, sections of fresh-frozen mouse tissues were fixed in 4% paraformaldehyde (PFA), acetylated with 1.33% triethanolamine (Fluka), 15 mM HCl, 0.25% acetic anhydride (Fluka), and blocked using a prehybridization solution (50% formamide, 5× Denhardt's, 250 g/ml baker's yeast RNA, 500 g/ml herring sperm DNA). This procedure was followed by hybridization of the denatured DIG-labeled RNA anti-sense probes to complementary RNA molecules on the sections at 70°C. DIG-labeled RNA sense probes also served as experimental controls. Slides were washed and blocked with 10% heat-inactivated sheep serum (HISS) for 1 h at room temperature. DIG-labeled hybrids were detected using an anti-DIG antibody conjugated with alkaline phosphatase, anti-digoxigenin-Ap Fab fragments (Roche Diagnostics). This strategy utilized a color reaction with 4-nitro blue tetrazolium chloride (NBT) and 5-bromo-4-chloro-3-indolyl phosphate (BCIP; Roche Diagnostics) as substrates, with hybridizations appearing as dark blue. Both cytoplasm and nucleus were counterstained as red by Fast Nuclear Red (DAKO, catalog no. S19863) and slides were mounted in Cytoseal 60 Mounting Medium (Stephens Scientific, Riverdale, NJ, USA).

Study subjects and mutation screening

In screening for gene mutations of *LPDL*, we first screened for polymorphisms in 60 hypertriglyceridemic Caucasian subjects with TG > 10 mmol/l and 10 normal controls (TG < 1 mmol/l). The high TG subjects had no mutations in *LPL*, *HL* and *EL*. The promoter, all exons, ∼100 bp of intron at each intron-exon boundary and 3′-UTR were screened using primers as follows: exon 1 forward (F)—AAA TCC TTC CCA CAA CCA CA, reverse (R)—TCC CAG AAT ACA GAC CAC ACT A; exon 2 F—ACC TTC AAC ATT GCA GTT GC, R—CAC TGC ATA TTG TAT AGC ACG; exon 3 F—AAA GTC TCT TTC CCG ATA TCC, R—GCA AAG TAA CTT CTG ATA C; exon 4 F—TAT GCA ATG TAA GGA GCT CTG, R—AGT GCC ATT TGA CAA TGC AG; exon 5 F—TTA TGC AAG ATA CTC ACC TG, R—AGT GCC ATT TGA CAA TGC AG; exon 6 F—AAA TGT ACT TGA ACA TGG C, R—ACA GTT TAG CTT CCA GCA GA; exon 7 F—GAT GGA AAT CCA ATT TCT AAT G, R—ATT TGA GTG GGT GCA AAG AAC; exon 8 F—CAT TTA CCA AAT GAG TCC TCT C, R—TTG TAT GGG ATA CTG AAG AAA GC; exon 9 F—ATT TTG TTC TCT GTG GCC TC, R—GTC TGA AAT ACA CAA TAA ACA G; exon 10 F—CCA TAT ATT TGT TCC AAC TC, R—TGG AAT GTT TAA CTG TAT GCA.

Silent and non-coding SNP allele frequencies were determined in 80 Caucasian subjects using either restriction digestion, undirectional genomic sequencing or allele-specific

methods, such purification with serum alkaline phosphatase and exonuclease I, followed by ddNTP primer extension and analysis on an ABI Prism 377 DNA Sequencer (PE Biosystems, Mississauga, Ontario, Canada). For some non-synonymous SNPs, allele frequencies were determined in additional subjects from various ethnic groups.

Estimates of pairwise linkage disequilibrium between the 12 SNP genotypes in 80 normal Caucasians were calculated as described (46). To test for association with clinical and quantitative traits, we aimed to select as few SNPs as possible for genotyping, based upon the following prioritization strategy: (1) the SNP changed the coding sequence; (2) the SNP minor allele frequency was >0.10; (3) non-coding SNPs had high information content (heterozygosity) and displayed strong linkage disequilibrium with other non-coding SNPs (representing 'haplotype blocks'). Based on this prioritization, the following four *LPDL* SNPs were genotyped in all samples: E431K, D444E, IVS2 [−74]C>T and 447C>T. Genotyping with these four SNPs essentially accounted for genotypes for all 12 SNPs because of linkage disequilibrium (data not shown).

We used our established approach to identify associations with clinical phenotypes (24–26), namely transformed plasma TG, total, LDL and HDL cholesterol in two independently ascertained, unrelated samples of healthy, normolipidemic Caucasians (Caucasian 1 and Caucasian 2) and a well-characterized sample of healthy Inuit (208 subjects) (26). The first sample of 174 Caucasians was 48.3% male and had mean (±SEM) age 50.1 ± 4.3 years. The second sample of 161 Caucasians was 42.0% male and had mean (±SEM) age 53.7 ± 5.8 years. A total of eight ANOVAs was performed as initial screening to identify significant associations: one ANOVA for each lipoprotein trait as the dependent variable in the Caucasian 1 and Inuit samples. Each ANOVA included age, sex and body mass index as independent covariates. The above four SNP genotypes were included as independent categorical variables in each ANOVA, with significance taken from the type III sums of squares (nominal $P < 0.05$). Type III sums of squares analysis is applicable to unbalanced study designs, and takes into account the effects of other independent variables included in the analysis. When a genotype was identified as being significantly associated with a plasma lipoprotein trait, we next performed a specific analysis to determine the best genetic model using ANOVA and including genetic model, age, sex and BMI as covariates. The least squares means with standard errors and levels of significance from these studies are shown in Table 3. We used a second independent Caucasian sample as a 'replication sample' (Caucasian 2), and found that the associations with IVS2 −74C>T were replicated, as shown in Table 3. We also determined allele frequencies of the above SNPs plus the other coding SNPs in 186 Caucasian patients with hypertriglyceridemia (TG>10 mmol/l, and no mutation in *LPL*, *HL* or *EL*) and 232 matched normolipidemic controls (TG < 1 mmol/l).

REFERENCES

1. Hide, W., Chan, L. and Li, W.-H. (1992) Structure and evolution of the lipase superfamily. *J. Lipid. Res.*, **33**, 167–178.
2. Goldberg, I.J. (1996) Lipoprotein lipase and lipolysis: central roles in lipoprotein metabolism and atherogenesis. *J. Lipid Res.*, **37**, 693–707.
3. Bensadoun, A. and Berryman, D.E. (1996) Genetics and molecular biology of hepatic lipase. *Curr. Opin. Lipidol.*, **7**, 77–81.
4. Jaye, M., Lynch, K.J., Krawiec, J., Marchadier, D., Maugeais, C., Doan, K., South, V., Amin, D., Oerrone, M. and Rader, D.J. (1999) A novel endothelial-derived lipase that modulates HDL metabolism. *Nat. Genet.*, **21**, 424–428.
5. Jin, W., Marchadier, D. and Rader, D.J. (2002) Lipases and HDL metabolism. *Trends Endocrinol. Metab.*, **13**, 174–178.
6. Holm, C., Kirchgessner, T.G., Svenson, K.L., Fredrikson, G., Nilsson, S., Miller, C.G., Shively, J.E., Heinzmann, C., Sparkes, R.S. and Mohandas, T. (1988) Hormone-sensitive lipase: sequence, expression, and chromosomal localization to 19 cent-q13.3. *Science*, **241**, 1503–1506.
7. Du, H., Sheriff, S., Bezerra, J., Leonova, T. and Grabowski, G.A. (1998) Molecular and enzymatic analyses of lysosomal acid lipase in cholesteryl ester storage disease. *Mol. Genet. Metab.*, **64**, 126–134.
8. Santamarina-Fojo, S. (1998) The familial chylomicronemia syndrome. *Endocrinol. Metab. Clin. N. Am.*, **27**, 551–567.
9. Hegele, R.A. (2001) Monogenic dyslipidemias: window on determinants of plasma lipoprotein metabolism. *Am. J. Hum. Genet.*, **69**, 1161–1177.
10. Busch, C.P. and Hegele, R.A. (2000) Variation of candidate genes in triglyceride metabolism. *J. Cardiovasc. Risk*, **7**, 309–315.
11. Goldberg, I.J. and Merkel, M. (2001) Lipoprotein lipase: physiology, biochemistry, and molecular biology. *Front. Biosci.*, **6**, D388–405.
12. Hegele, R.A., Little, J.A., Vezina, C., Maguire, G.F., Tu, L., Wolever, T.S., Jenkins, D.J. and Connelly, P.W. (1993) Hepatic lipase deficiency: clinical, biochemical, and molecular genetic characteristics. *Arterioscler. Thromb.*, **13**, 720–728.
13. Cohen, J.C., Vega, G.L. and Grundy, S.M. (1999) Hepatic lipase: new insights from genetic and metabolic studies. *Curr. Opin. Lipidol.*, **10**, 259–267.
14. Kawano, K., Qin, S., Vieu, C., Collet, X. and Jiang, X.C. (2002) Role of hepatic lipase and scavenger receptor BI in clearing phospholipid/free cholesterol-rich lipoproteins in PLTP-deficient mice. *Biochim. Biophys. Acta*, **1583**, 133–140.
15. deLemos, A.S., Wolfe, M.L., Long, C.J., Sivapackianathan, R. and Rader, D.J. (2002) Identification of genetic variants in endothelial lipase in persons with elevated high-density lipoprotein cholesterol. *Circulation*, **106**, 1321–1326.
16. Wen, X.-Y., Bryce, D.M. and Breitman, M.L. (1998) Characterization of lpd (lipid defect): a novel mutation on mouse chromosome 16 associated with a defect in triglyceride metabolism. *Hum. Mol. Genet.*, **7**, 743–750.
17. Wen, X.-Y., Stewart, A.K., Skaug, J., Wei, E. and Tsui, L.C. (2001) Murine phosphatidylserine-specific phospholipase A1 (Ps-pla1) maps to chromosome 16 but is distinct from the lpd (lipid defect) locus. *Mammal. Genome*, **12**, 129–132.
18. Jin, W., Broedl, U., Monajemi, H., Glick, J. and Rader, D. (2002) Lipase H, a new member of the triglyceride lipase family synthesized by the intestine. *Genomics*, **80**, 268–273.
19. Emmerich, J., Beg, O.U., Peterson, J., Previato, L., Brunzell, J.D., Brewer, H.B. Jr. and Santamarina-Fojo, S. (1992) Human lipoprotein lipase. Analysis of the catalytic triad by site-directed mutagenesis of Ser-132, Asp-156, and His-241. *J. Biol. Chem.*, **267**, 4161–4165.
20. Dugi, K.A., Dichek, H.L. and Santamarina-Fojo, S. (1995) Human hepatic and lipoprotein lipase: the loop covering the catalytic site mediates lipase substrate specificity. *J. Biol. Chem.*, **270**, 25396–25401.
21. van Tilbeurgh, H., Roussel, A., Lalouel, J.M. and Cambillau, C. (1994) Lipoprotein lipase. Molecular model based on the pancreatic lipase X-ray structure: consequences for heparin binding and catalysis. *J. Biol. Chem.*, **269**, 4626–4633.
22. Henikoff, S. and Henikoff, J.G. (1992) Amino acid substitution matrices from protein blocks. *Proc. Natl Acad. Sci. USA*, **89**, 10915–10919.
23. Lowe, M.E. (1997) Molecular mechanisms of rat and human pancreatic triglyceride lipases. *J. Nutr.*, **127**, 549–557.
24. Hegele, R.A., Evans, A., Tu, L., Ip, G., Brunt, J.H. and Connelly, P.W. (1994) A gene-gender interaction affecting plasma lipoproteins in a genetic isolate. *Arterioscler. Thromb.*, **14**, 671–678.
25. Hegele, R.A., Ramdath, D.D., Ban, M.R., Carruthers, M.N., Carrington, C.V. and Cao, H. (2001) Polymorphisms in *PNLIP*, encoding pancreatic lipase, and associations with metabolic traits. *J. Hum. Genet.*, **46**, 320–324.
26. Hegele, R.A., Wang, J., Harris, S.B., Brunt, J.H., Young, T.K., Hanley, A.J., Zinman, B., Connelly, P.W., and Anderson, C.M. (2001) Variable association between genetic variation in the CYP7 gene promoter and plasma lipoproteins in three Canadian populations. *Atherosclerosis*, **154**, 579–587.

27. Woychik, R.P., Maas, R.L., Zeller, R., Vogt, T.F. and Leder, P. (1990) 'Formins': proteins deduced from the alternative transcripts of the limb deformity gene. *Nature*, **346**, 850–858.
28. Sato, T., Aoki, J., Nagai, Y., Dohame, N., Takio, K., Doi, T., Arai, H. and Inoue, K. (1997) Serine phospholipid-specific phospholipase A that is secreted from activated platelets. *J. Biol. Chem.*, **272**, 2192–2198.
29. Wang, J., Wen, X.-Y., Stewart, A.K. and Hegele, R.A. (2002) Polymorphisms in the gene encoding phosphatidylserine-specific phospholipase A1 (PS-PLA1), *J. Hum. Genet.*, **47**, 611–613.
30. Igarashi, K., Kaneda, M., Yamaji, A., Saido, T.C., Kikkawa, U., Ono, Y., Inoue, K. and Umeda, M. (1995) A novel phosphatidylserine-binding peptide motif defined by an anti-idiotypic monoclonal antibody. Localization of phosphatidylserine-specific binding sites on protein kinase C and phosphatidylserine decarboxylase. *J. Biol. Chem.*, **270**, 29075–29078.
31. Hirata, K., Dichek, H.L., Cioffi, J.A., Choi, S.Y., Leeper, N.J., Quintana, L., Kronmal, G.S., Cooper, A.D. and Quertermous, T. (1999) Cloning of a unique lipase from endothelial cells extends the lipase gene family. *J. Biol. Chem.*, **274**, 14170–14175.
32. Mairal, A., Melaine, N., Laurell, H., Grober, J., Holst, L.S., Guillaudeux, T., Holm, C., Jegou, B. and Langin, D. (2002) Characterization of a novel testicular form of human hormone-sensitive lipase. *Biochem. Biophys. Res. Commun.*, **291**, 286–290.
33. Haemmerle, G., Zimmermann, R., Strauss, J.G., Kratky, D., Riederer, M., Knipping, G. and Zechner, R. (2002) Hormone-sensitive lipase deficiency in mice changes the plasma lipid profile by affecting the tissue-specific expression pattern of lipoprotein lipase in adipose tissue and muscle. *J. Biol. Chem.*, **277**, 12946–12952.
34. Haemmerle, G., Zimmermann, R., Hayn, M., Theussl, C., Waeg, G., Wagner, E., Sattler, W., Magin, T.M., Wagner, E.F. and Zechner, R. (2002) Hormone-sensitive lipase deficiency in mice causes diglyceride accumulation in adipose tissue, muscle, and testis. *J. Biol. Chem.*, **277**, 4806–4815.
35. Osuga, J., Ishibashi, S., Oka, T., Yagyu, H., Tozawa, R., Fujimoto, A., Shionoiri, F., Yahagi, N., Kraemer, F.B., Tsutsumi, O. and Yamada, N. (2000) Targeted disruption of hormone-sensitive lipase results in male sterility and adipocyte hypertrophy, but not in obesity. *Proc. Natl Acad. Sci. USA.*, **97**, 787–792.
36. Peterfy, M., Phan, J., Xu, P. and Reue, K. (2001) Lipodystrophy in the fld mouse results from mutation of a new gene encoding a nuclear protein, lipin. *Nat. Genet.*, **27**, 121–124.
37. Claudio, J.O., Zhu, Y.X., Benn, S.J., Shukla, A.H., McGlade, C.J., Falcioni, N. and Stewart, A.K. (2001) HACS1 encodes a novel SH3-SAM adaptor protein differentially expressed in normal and malignant hematopoietic cells. *Oncogene*, **20**, 5373–5377.
38. Stengard, J.H., Clark, A.G., Weiss, K.M., Kardia, S., Nickerson, D.A., Salomaa, V., Ehnholm, C., Boerwinkle, E. and Sing, C.F. (2002) Contributions of 18 additional DNA sequence variations in the gene encoding apolipoprotein E to explaining variation in quantitative measures of lipid metabolism. *Am. J. Hum. Genet.*, **71**, 501–517.
39. Cohen, J.C. (2003) Endothelial lipase: direct evidence for a role in HDL metabolism. *J. Clin. Invest.*, **111**, 318–321.
40. Ishida, T., Choi, S., Kundu, R.K., Hirata, K., Rubin, E.M., Cooper, A.D. and Quertermous, T. (2003) Endothelial lipase is a major determinant of HDL level. *J. Clin. Invest.*, **111**, 347–355.
41. Jin, W., Millar, J.S., Broedl, U., Glick, J.M. and Rader, D.J. (2003) Inhibition of endothelial lipase causes increased HDL cholesterol levels *in vivo*. *J. Clin. Invest.*, **111**, 357–362.
42. Arya, R., Duggirala, R., Almasy, L., Rainwater, D.L., Mahaney, M.C., Cole, S., Dyer, T.D., Williams, K., Leach, R.J., Hixson, J.E. *et al.* (2002) Linkage of high-density lipoprotein-cholesterol concentrations to a locus on chromosome 9p in Mexican Americans. *Nat. Genet.*, **30**, 102–105.
43. Broeckel, U., Hengstenberg, C., Mayer, B., Holmer, S., Martin, L.J., Comuzzie, A.G., Blangero, J., Nurnberg, P., Reis, A., Riegger, G.A. *et al.* (2002) A comprehensive linkage analysis for myocardial infarction and its related risk factors. *Nat. Genet.*, **30**, 210–214.
44. Rossant, J. and McKerlie, C. (2001) Mouse-based phenogenomics for modelling human disease. *Trends. Mol. Med.*, **7**, 502–507.
45. Schaeren-Wiemers, N. and Gerfin-Moser, A. (1993) A single protocol to detect transcripts of various types and expression levels in neural tissue and cultured cells: *in situ* hybridization using digoxigenin-labelled cRNA probes. *Histochemistry*, **100**, 431–440.
46. Hegele, R.A., Plaetke, R. and Lalouel, J.M. (1990) Linkage disequilibrium between DNA markers at the low-density lipoprotein receptor gene. *Genet. Epidemiol.*, **7**, 69–81.